

Dirhodium Formamidinate Compounds with Bidentate Nitrogen Chelating Ligands

Helen T. Chifotides, Kemal V. Catalan, and Kim R. Dunbar*

Department of Chemistry, Texas A&M University, College Station, Texas 77843

Received June 27, 2003

The reactions of $[\text{Rh}_2(\text{DTolF})_2(\text{CH}_3\text{CN})_6][\text{BF}_4]_2$ (**1**) (DTolF = *N,N'*-di-*p*-tolylformamidinate) with 2,2'-bipyridine (bpy) and 1,10-phenanthroline (phen) proceed with substitution of CH_3CN molecules to give products with the N–N ligands chelating in an equatorial–equatorial (*eq–eq*) fashion. Compound **1** reacts with 1 equiv of bpy to yield a mixture of $[\text{Rh}_2(\text{DTolF})_2(\text{bpy})(\text{CH}_3\text{CN})_3][\text{BF}_4]_2 \cdot (\text{CH}_3)_2\text{CO}$ (**2a**) and $[\text{Rh}_2(\text{DTolF})_2(\text{bpy})(\text{CH}_3\text{CN})_4][\text{BF}_4]_2$ (**2b**). Compound **2a** crystallizes in the monoclinic space group $P2_1/n$ with $a = 13.5856(2) \text{ \AA}$, $b = 18.0402(2) \text{ \AA}$, $c = 21.4791(3) \text{ \AA}$; $\alpha = 90^\circ$, $\beta = 101.044(1)^\circ$, $\gamma = 90^\circ$; $V = 5167.27(12) \text{ \AA}^3$, $Z = 4$, $R = 0.0531$, and $R_w = 0.0948$. Compound **2b** crystallizes in the monoclinic space group $P2_1/n$ with $a = 10.9339(2) \text{ \AA}$, $b = 24.4858(1) \text{ \AA}$, $c = 19.4874(3) \text{ \AA}$; $\alpha = 90^\circ$, $\beta = 94.329(1)^\circ$, $\gamma = 90^\circ$; $V = 5202.38(13) \text{ \AA}^3$, $Z = 4$, $R = 0.0459$, and $R_w = 0.1140$. The reaction of compound **1** with 2 equiv of bpy affords $[\text{Rh}_2(\text{DTolF})_2(\text{bpy})_2(\text{CH}_3\text{CN})][\text{BF}_4]_2$ (**3**) which crystallizes in the monoclinic space group $P2_1/a$ with $a = 19.4534(4) \text{ \AA}$, $b = 13.8298(3) \text{ \AA}$, $c = 19.8218(5) \text{ \AA}$; $\alpha = 90^\circ$, $\beta = 109.189(1)^\circ$, $\gamma = 90^\circ$; $V = 5036.5(2) \text{ \AA}^3$, $Z = 4$, $R = 0.0589$, and $R_w = 0.0860$. Compound **1** reacts with 1 equiv of phen to form $[\text{Rh}_2(\text{DTolF})_2(\text{phen})(\text{CH}_3\text{CN})_3][\text{BF}_4]_2 \cdot 2\text{C}_2\text{H}_5\text{OC}_2\text{H}_5$ (**4**) which crystallizes in the triclinic space group $P\bar{1}$ with $a = 12.6346(2) \text{ \AA}$, $b = 13.5872(2) \text{ \AA}$, $c = 19.0597(3) \text{ \AA}$; $\alpha = 71.948(1)^\circ$, $\beta = 73.631(1)^\circ$, $\gamma = 71.380(1)^\circ$; $V = 2886.70(8) \text{ \AA}^3$, $Z = 2$, $R = 0.0445$, and $R_w = 0.1207$. A notable feature of the cations in **2a**, **3**, and **4** is the presence of only one axial (*ax*) CH_3CN ligand, a fact that can be attributed to the steric effect of the formamidinate bridging ligands. Compounds **2a**, **2b**, **3**, and **4** were fully characterized by X-ray crystallography and ^1H NMR spectroscopy, whereas $[\text{Rh}_2(\text{DTolF})_2(\text{phen})_2(\text{CH}_3\text{CN})_2][\text{BF}_4]_2$ (**5**) was characterized by ^1H NMR spectroscopy.

Introduction

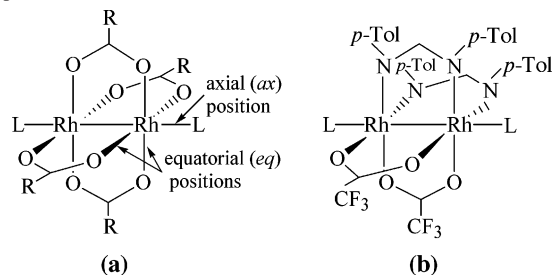
In the last few decades, dinuclear metal–metal bonded complexes of rhodium have been shown to exhibit appreciable carcinostatic activity against various tumor cell lines. Although the exact mechanism of antitumor activity is not known, previous research supports the conclusions that dirhodium compounds inhibit DNA replication, *in vitro* transcription, protein synthesis, and promote DNA photocleavage.^{1,2} The dirhodium tetracarboxylate compounds of the type $\text{Rh}_2(\text{O}_2\text{CR})_4\text{L}_2$ ($\text{R} = \text{Me, Et, Pr}$; $\text{L} = \text{solvent}$)³ (Chart 1a) have been found to exhibit carcinostatic activity against the Ehrlich ascites, sarcoma 180 and P388,¹ whereas the mixed formamidinate/carboxylate compounds $\text{Rh}_2(\text{DTolF})_2(\text{O}_2\text{CCF}_3)_2(\text{H}_2\text{O})_2$ (DTolF = *N,N'*-di-*p*-tolylformamidinate)⁴ (Chart 1b) exhibit *in vivo* carcinostatic activity against Yoshida ascites and T8 sarcoma cells comparable to *cis*- $\text{PtCl}_2(\text{NH}_3)_2$, but with considerably reduced toxicity.⁵ More-

over, it has been recently demonstrated that the compounds $[\text{Rh}_2(\text{O}_2\text{CCH}_3)_2(\text{N–N})_2(\text{H}_2\text{O})_2]^{2+}$ {N–N = 2,2'-bipyridine (bpy) or 1,10-phenanthroline (phen)} exhibit higher carci-

- (1) (a) Erck, A.; Rainen, L.; Whaleyman, J.; Chang, I.; Kimball, A. P.; Bear, J. L. *Proc. Soc. Exp. Biol. Med.* **1974**, *145*, 1278. (b) Bear, J. L.; Gray, H. B.; Rainen, L.; Chang, I. M.; Howard, R.; Serio, G.; Kimball, A. P. *Cancer Chemother. Rep. Part I* **1975**, *59*, 611. (c) Howard, R. A.; Spring, T. G.; Bear, J. L. *Cancer Res.* **1976**, *36*, 4402. (d) Erck, A.; Sherwood, E.; Bear, J. L.; Kimball, A. P. *Cancer Res.* **1976**, *36*, 2204. (e) Howard, R. A.; Sherwood, E.; Erck, A.; Kimball, A. P.; Bear, J. L. *J. Med. Chem.* **1977**, *20*, 943. (f) Howard, R. A.; Kimball, A. P.; Bear, J. L. *Cancer Res.* **1979**, *39*, 2568. (g) Rao, P. N.; Smith, M. L.; Pathak, S.; Howard, R. A.; Bear, J. L. *J. Natl. Cancer Inst.* **1980**, *64*, 905. (h) Hall, L. M.; Speer, R. J.; Ridgway, H. J. *J. Clin. Hematol. Oncol.* **1980**, *10*, 25. (i) Bear, J. L. In *Precious Metals 1985: Proceedings of the Ninth International Precious Metals Conference*; Zysk, E. D., Bonucci, J. A., Eds.; International Precious Metals: Allentown, PA, 1986; pp 337–344.
- (2) (a) Fu, P. K.-L.; Bradley, P. M.; Turro, C. *Inorg. Chem.* **2001**, *40*, 2476. (b) Sorasaneene, K.; Fu, P. K.-L.; Angeles-Boza, A. M.; Dunbar, K. R.; Turro, C. *Inorg. Chem.* **2003**, *42*, 1267. (c) Chifotides, H. T.; Fu, P. K.-L.; Dunbar, K. R.; Turro, C. *Inorg. Chem.*, submitted for publication, 2003.
- (3) Cotton, F. A.; Walton, R. A. *Multiple Bonds Between Metal Atoms*; Clarendon Press: Oxford, 1993; Chapter 7, pp 431–501.

* To whom correspondence should be addressed. E-mail: dunbar@mail.chem.tamu.edu.

Chart 1. Structure of Dirhodium Metal–Metal Bonded (a) Tetracarboxylate and (b) Mixed Formamidinate/Trifluoroacetate Compounds



nostatic activity than the dirhodium tetracarboxylate adducts against human oral carcinoma KB cells *in vitro*;⁶ the latter have also been reported to be active cytostatic and antibacterial agents⁷ and to effectively bind to human serum albumin.⁸

Apart from the well-established preference for axial (*ax*) binding of adenine to the dirhodium core,⁹ recent findings in our laboratories have *unequivocally* established that equatorial (*eq*) purine interactions are also possible. Model dirhodium compounds with 9-ethylguanine and 9-ethyladenine revealed the presence of bridging or chelating binding modes for the purines *via* the *N7/O6* or *N7/N6* sites, respectively.^{10–12} Dirhodium adducts with the DNA fragments d(GpG) and d(pGpG) have also shown adjacent *head-to-head* purine ligands bound through *N7/O6* to *cis eq* positions of the rhodium centers.¹³ In addition, studies performed by mass spectrometry have established that dirhodium bis-acetate units form adducts with AA and GG containing DNA dodecamers.¹⁴

Prior to establishing that adjacent DNA nucleobases bind to the dirhodium core, bpy was used as a single bidentate nitrogen chelate to mimic binding of two adjacent DNA bases

to $\text{Rh}_2(\text{O}_2\text{CR})_4\text{L}_2$ ($\text{R} = \text{Me, Et, Ph}$ or CF_3 ; $\text{L} =$ donor molecule). The relevant studies demonstrated the ability of single N–N chelating ligands to interact with the dirhodium core through several binding modes; these include *ax–eq* and *eq–eq* interactions, and their identification has provided valuable information *vis-à-vis* the mechanism by which DNA bases attach to the dirhodium core.¹⁵ Related studies involving the reactions of $\text{Rh}_2(\text{DTolF})_2(\text{O}_2\text{CCF}_3)_2(\text{H}_2\text{O})_2$ with bpy and phen led to the conclusion that similar binding modes are possible for these compounds with N–N chelates, although no solid-state structures were obtained.¹⁶

Herein, we describe the syntheses and single-crystal X-ray structural determinations of compounds that contain bpy or phen bound to the *cis*- $[\text{Rh}_2(\text{DTolF})_2]^{2+}$ core. These investigations indicate that the dirhodium (II,II) formamidinate compounds preferentially form *eq–eq* adducts with these N–N chelating ligands and crystallize with unoccupied *ax* sites even in the presence of excess donor solvent molecules. The ¹H NMR spectroscopic and cyclic voltammetric data are in accord with the solid-state structures determined by single-crystal X-ray diffraction studies.

Experimental Section

Starting Materials. The partially solvated compound $[\text{Rh}_2(\text{DTolF})_2(\text{CH}_3\text{CN})_6][\text{BF}_4]_2$ (**1**) was prepared by literature procedures.¹¹ The reagents 2,2'-bipyridine (bpy) and 1,10-phenanthroline monohydrate (phen) were purchased from Aldrich. The compound 9-ethylguanine (9-EtGH) was purchased from Sigma, whereas 9-ethyladenine (9-EtAH) was prepared by reported literature procedures.¹¹ All solvents were predried from 4 Å molecular sieves with the exception of acetone and acetonitrile which were predried over 3 Å molecular sieves and distilled under a nitrogen atmosphere. Diethyl ether and toluene were distilled from Na/K, and methylene chloride was distilled from P₂O₅. Acetonitrile used for electrochemical measurements was further dried by being passed through an activated alumina column under Ar. All manipulations were performed under inert atmospheric conditions using standard Schlenk-line techniques unless otherwise stated.

Syntheses. Preparation of $[\text{Rh}_2(\text{DTolF})_2(\text{bpy})(\text{CH}_3\text{CN})_{3,4}][\text{BF}_4]_2$ (2**).** A green solution of $[\text{Rh}_2(\text{DTolF})_2(\text{CH}_3\text{CN})_6][\text{BF}_4]_2$ (**1**) (92 mg, 0.0857 mmol) in acetone (5 mL) was treated with a solution of bpy (13.4 mg, 0.0858 mmol) in acetone (2 mL). The reaction mixture was stirred at r.t. for ~24 h, after which time the reaction solvent was concentrated to half the original volume under reduced pressure. The product was precipitated from solution by addition of diethyl ether (~10 mL) and collected by filtration in air to yield 88 mg (0.0767 mmol, 89.5% yield). Anal. Calcd for C₄₆H₄₇B₂F₈N₉-Rh₂ (**2a** without solvent): C, 49.98; H, 4.29; N, 11.41. Anal. Calcd for bulk powder: C, 49.99; H, 4.35; N, 11.92. Single crystals of

- (4) Piraino, P.; Bruno, G.; Tresoldi, G.; Lo Schiavo, S.; Zanello, P. *Inorg. Chem.* **1987**, *26*, 91.
 (5) Fimiani, V.; Ainis, T.; Cavallaro, A.; Piraino, P. *J. Chemother. (Florence)* **1990**, *2*, 319.
 (6) Pruchnik, F.; Dus, D. *J. Inorg. Biochem.* **1996**, *61*, 55.
 (7) (a) Pruchnik, F. P.; Bien, M.; Lachowicz, T.; *Met. Based Drugs* **1996**, *3*, 185. (b) Pruchnik, F. P.; Kluczevska, G.; Wilczok, A.; Mazurek, U.; Wilczok, T. *J. Inorg. Biochem.* **1997**, *65*, 25. (c) Bien, M.; Pruchnik, F. P.; Seniuk, A.; Lachowicz, T. M.; Jakimowicz, P. *J. Inorg. Biochem.* **1999**, *73*, 49.
 (8) Trynda-Lemiesz, L.; Pruchnik, F. P. *J. Inorg. Biochem.* **1997**, *66*, 187.
 (9) (a) Rainen, L.; Howard, R. A.; Kimball, A. P.; Bear, J. L. *Inorg. Chem.* **1975**, *14*, 2752. (b) Pneumatikakis, G.; Hadjiliadis, N. *J. Chem. Soc., Dalton Trans.* **1979**, 596. (c) Farrell, N. *J. Chem. Soc., Chem. Commun.* **1980**, 1014. (d) Farrell, N. *J. Inorg. Biochem.* **1981**, *14*, 261. (e) Rubin, J. R.; Sundaralingam, M. *J. Biomol. Struct. Dyn.* **1984**, *2*, 525. (f) Rubin, J. R.; Haromy, T. P.; Sundaralingam, M. *Acta Crystallogr.* **1991**, *C47*, 1712. (g) Aoki, K.; Salam, M. A. *Inorg. Chim. Acta* **2002**, *339*, 427.
 (10) (a) Dunbar, K. R.; Matonic, J. H.; Saharan, V. P.; Crawford, C. A.; Christou, G. *J. Am. Chem. Soc.* **1994**, *116*, 2201. (b) Day, E. F.; Crawford, C. A.; Foltling, K.; Dunbar, K. R.; Christou, G. *J. Am. Chem. Soc.* **1994**, *116*, 9339. (c) Crawford, C. A.; Day, E. F.; Saharan, V. P.; Foltling, K.; Huffman, J. C.; Dunbar, K. R.; Christou, G. *Chem. Commun.* **1996**, 1113.
 (11) (a) Catalan, K. V.; Mendiola, D. J.; Ward, D. L.; Dunbar, K. R. *Inorg. Chem.* **1997**, *36*, 2458. (b) Catalan, K. V.; Hess, J. S.; Maloney, M. M.; Mendiola, D. J.; Ward, D. L.; Dunbar, K. R. *Inorg. Chem.* **1999**, *38*, 3904.
 (12) Phillips, S. L.; Christou, G.; Huffman, J. C.; Olmstead, M. M. *Abstr. Pap. Am. Chem. Soc.* **2001**, 221, INOR–524.
 (13) (a) Chifotides, H. T.; Koshlap, K. M.; Pérez, L. M.; Dunbar, K. R. *J. Am. Chem. Soc.* **2003**, *125*, 10703. (b) Chifotides, H. T.; Koshlap, K. M.; Pérez, L. M.; Dunbar, K. R. *J. Am. Chem. Soc.* **2003**, *125*, 10714.

- (14) (a) Asara, J. M.; Hess, J. S.; Lozada, E.; Dunbar, K. R.; Allison, J. J. *J. Am. Chem. Soc.* **2000**, *122*, 8. (b) Chifotides, H.; Koomen, J. M.; Mijeong K.; Tichy, S. E.; Dunbar, K. R.; Russell, D. H., manuscript in preparation.
 (15) (a) Perlepes, S. P.; Huffman, J. C.; Matonic, J. H.; Dunbar, K. R.; Christou, G. *J. Am. Chem. Soc.* **1991**, *113*, 2770. (b) Crawford, C. A.; Matonic, J. H.; Streib, W. E.; Huffman, J. C.; Dunbar, K. R.; Christou, G. *J. Inorg. Chem.* **1993**, *32*, 3125. (c) Crawford, C. A.; Matonic, J. H.; Huffman, J. C.; Foltling, K.; Dunbar, K. R.; Christou, G. *J. Inorg. Chem.* **1997**, *36*, 2361.
 (16) Schiavo, S. L.; Sinicropi, M. S.; Tresoldi, G.; Arena, C. G.; Piraino, P. *J. Chem. Soc., Dalton Trans.* **1994**, 1517 and references therein.

Table 1. Crystallographic Data for [Rh₂(DTolF)₂(bpy)(CH₃CN)₃][BF₄]₂·(CH₃)₂CO (**2a**), [Rh₂(DTolF)₂(bpy)(CH₃CN)₄][BF₄]₂ (**2b**), [Rh₂(DTolF)₂(bpy)₂(CH₃CN)][BF₄]₂ (**3**), and [Rh₂(DTolF)₂(phen)(CH₃CN)₃][BF₄]₂·2C₂H₅OC₂H₅ (**4**)

| | 2a | 2b | 3 | 4 |
|--|---|---|--|---|
| formula ^a | C ₄₉ H ₅₃ B ₂ F ₈ N ₉ ORh ₂ | C ₄₈ H ₅₀ B ₂ F ₈ N ₁₀ Rh ₂ | C ₅₂ H ₄₉ B ₂ F ₈ N ₉ Rh ₂ | C ₅₆ H ₆₇ B ₂ F ₈ N ₉ O ₂ Rh ₂ |
| fw, g/mol | 1163.44 | 1146.42 | 1179.44 | 1277.63 |
| crystal system | monoclinic | monoclinic | monoclinic | triclinic |
| space group | <i>P</i> 2 ₁ / <i>n</i> | <i>P</i> 2 ₁ / <i>n</i> | <i>P</i> 2 ₁ / <i>a</i> | <i>P</i> $\bar{1}$ |
| <i>a</i> , Å | 13.5856(2) | 10.9339(2) | 19.4534(4) | 12.6346(2) |
| <i>b</i> , Å | 18.0420(2) | 24.4858(1) | 13.8298(3) | 13.5872(2) |
| <i>c</i> , Å | 21.4791(3) | 19.4874(3) | 19.8218(5) | 19.0597(3) |
| α , deg | 90 | 90 | 90 | 71.948(1) |
| β , deg | 101.044(1) | 94.329(1) | 109.189(1) | 73.631(1) |
| γ , deg | 90 | 90 | 90 | 71.380(1) |
| <i>V</i> , Å ³ | 5167.27(12) | 5202.38(13) | 5036.5(2) | 2886.70(8) |
| <i>Z</i> | 4 | 4 | 4 | 2 |
| <i>T</i> , K | 173(2) | 173(2) | 173(2) | 173(2) |
| <i>D_c</i> , g/cm ³ | 1.496 | 1.464 | 1.555 | 1.474 |
| μ_{Mo} , cm ⁻³ | 0.713 | 0.706 | 0.0731 | 0.652 |
| <i>N</i> | 10600 | 5446 | 11822 | 12408 |
| <i>N_o</i> ^b | 6770 | 4267 | 7079 | 9697 |
| <i>R^c</i> | 0.0531 | 0.0459 | 0.0589 | 0.0445 |
| <i>R_w</i> ^d | 0.0948 | 0.1140 | 0.0860 | 0.1207 |

^a Including solvent molecules. ^b $I > 2\sigma(I)$. ^c $R = \sum||F_o| - |F_c||/\sum|F_o|$. ^d $R_w = \{\sum[w(F_o^2 - F_c^2)^2]/\sum[w(F_o^2)^2]\}^{1/2}$.

2a were grown from an acetone solution layered with ethyl acetate. Single crystals of **2b** were grown from an acetonitrile solution of the compound layered with diethyl ether. ¹H NMR (CD₃CN-*d*₃) δ ppm: 1.95 (s, *ax*-CH₃CN), 2.22 (s, tolyl CH₃), 2.25 (s, *eq*-CH₃-CN), 6.99 (m, tolyl), 7.77 (t, bpy), 7.83 (t, ³*J*_{Rh-H} = 3.6 Hz, NCHN), 8.24 (t, bpy), 8.50 (d, bpy), 9.06 (d, bpy).

The previous reaction was performed in CH₃CN at r.t. with the following result: a dark orange-red solution of [Rh₂(DTolF)₂(CH₃-CN)₆][BF₄]₂ (**1**) (75.0 mg, 0.0692 mmol) in acetonitrile (4 mL) was added via cannula to a solution of bpy (10.8 mg, 0.0691 mmol) in acetonitrile (5 mL). The mixture was stirred until the brown-green solution was concentrated to ~4 mL under reduced pressure (24 h). A solid was precipitated by addition of hexanes (1 mL) and diethyl ether (5 mL). The resulting microcrystalline material was collected by suction filtration in air and dried *in vacuo*. The product was identified by ¹H NMR spectroscopy as a mixture of **2b** and **3** (*vide infra*).

Preparation of [Rh₂(DTolF)₂(bpy)₂(CH₃CN)][BF₄]₂ (3**).** A solution of **1** (105 mg, 0.0968 mmol) in CH₃CN (7 mL) was treated with bpy (30.24 mg, 0.1936 mmol) and refluxed for ~48 h. The reaction mixture was cooled to r.t., and diethyl ether (15 mL) was added to yield microcrystals (73 mg, 0.0620 mmol, yield 64%) which were collected by filtration in air. Anal. Calcd for C₅₂H₄₉B₂F₈N₉Rh₂: C, 52.95; H, 4.19; N, 10.69. Found: C, 53.72; H, 4.12; N, 10.90. X-ray quality single crystals were grown by careful layering of an acetone solution of **3** with ethyl acetate. ¹H NMR (CD₃CN-*d*₃) δ ppm: 1.95 (s, *ax*-CH₃CN), 2.23 (s, tolyl CH₃), 6.99 (m, tolyl), 7.29 (t, bpy), 7.79 (d, bpy), 7.86 (t, bpy), 8.17 (t, ³*J*_{Rh-H} = 3.6 Hz, NCHN), 8.38 (d, bpy).

Preparation of [Rh₂(DTolF)₂(phen)(CH₃CN)₃][BF₄]₂·2C₂H₅-OC₂H₅ (4**).** A mixture of **1** (100 mg, 0.0934 mmol) and 1,10-phenanthroline monohydrate (18.3 mg, 0.0921 mmol) in CH₂Cl₂ (5 mL) was stirred for ~72 h at r.t. The mixture was filtered through Celite in air to remove undissolved materials and concentrated to half the original volume. The green product was isolated after addition of diethyl ether, dried *in vacuo*, and recrystallized from methylene chloride and diethyl ether (0.0832 mmol, 94 mg, yield 90%). Anal. Calcd for C₄₈H₄₇B₂F₈N₉Rh₂: C, 51.04; H, 4.19; N, 11.16. Found: C, 51.00; H, 4.20; N, 11.20. Single crystals were grown by layering a methylene chloride solution of the compound with ethyl acetate. ¹H NMR (CD₃CN-*d*₃) δ ppm: 1.95 (s, *ax*-CH₃-CN), 2.25 (s, tolyl CH₃), 2.51 (s, *eq*-CH₃CN), 6.99 (m, tolyl), 7.51

(t, ³*J*_{Rh-H} = 3.6 Hz, NCHN), 7.92 (q, phen), 8.06 (s, phen), 8.60 (d, phen), 9.05 (d, phen).

Preparation of [Rh₂(DTolF)₂(phen)₂(CH₃CN)₂][BF₄]₂ (5**).** A mixture of **1** (75.0 mg, 0.0701 mmol) and 1,10-phenanthroline monohydrate (27.7 mg, 0.139 mmol) in CH₃CN (10 mL) was heated to reflux for ~64 h. The green solution was concentrated to half the original volume, and the product was isolated as microcrystals after addition of diethyl ether. The microcrystals were collected by filtration in air and dried *in vacuo* (0.047 mmol, 60 mg, yield 67%). Anal. Calcd for C₅₈H₅₂B₂F₈N₁₀Rh₂: C, 54.91; H, 4.13; N, 11.04. Found: C, 54.80; H, 4.15; N, 11.16. X-ray quality single crystals were grown by careful layering of an acetone solution of **5** with ethyl acetate, but their poor quality did not permit full X-ray structural characterization. ¹H NMR (CD₃CN-*d*₃) δ ppm: 1.95 (s, *ax*-CH₃CN), 2.24 (s, tolyl CH₃), 7.05 (m, tolyl), 7.52 (q, phen), 7.63 (s, phen), 8.16 (d, phen), 8.30 (t, ³*J*_{Rh-H} = 3.6 Hz, NCHN), 8.57 (d, phen).

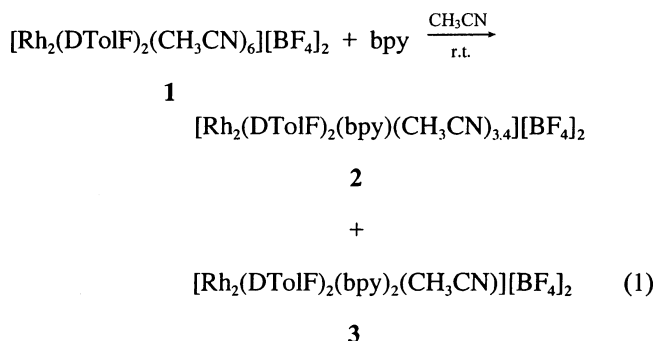
Physical Measurements. One- (1D) and two- (2D) dimensional ¹H NMR spectroscopic data were collected on a 300 or 500 MHz Varian spectrometer. Chemical shifts were referenced relative to the residual proton impurities of the deuterated solvent (CD₃CN-*d*₃). Electrochemical measurements were performed by using an EG&G Princeton Applied Research model 362 scanning potentiostat in conjunction with a Soltec model VP-6424S X-Y recorder. Cyclic voltammetric experiments for **2**, **3**, and **4** were carried out at r.t. in CH₃CN with 0.1 M tetra-*n*-butylammonium tetrafluoroborate as supporting electrolyte. *E*_{1/2} values, determined as (*E*_{p,a} + *E*_{p,c})/2, were referenced to the Ag/AgCl electrode without correction for junction potentials. The Cp₂Fe/[Cp₂Fe]⁺ couple occurs at *E*_{1/2} = +0.45 V under the same conditions of the cyclic voltammograms for compounds **2** and **3** in CH₃CN.

Single-Crystal X-ray Diffraction Studies. X-ray data sets for **2a**, **2b**, **3**, and **4** were collected on a Bruker AXS SMART diffractometer with graphite monochromated Mo K α radiation (average λ_{α} = 0.71073 Å). A hemisphere of crystallographic data was collected for each of **2b**, **3**, and **4**, whereas one-quarter of a sphere was collected for **2a**. The frames were integrated with the Bruker AXS SAINT software package, and the data was corrected for absorption using the SADABS program in the same software package.¹⁷ The structures of **2b** and **4** were solved by Patterson methods using the SHELXS program in the Bruker AXS SHELXTL v. 5.05 software.¹⁸ The structure of **2a** was solved by direct methods

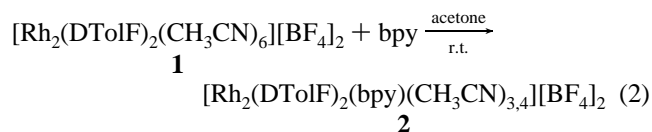
using the same software package. The structure of **3** was solved by Patterson methods using the SHELXS-86 program in the Texsan software package.¹⁹ All of the structures were refined by full-matrix least-squares calculations on F^2 using the SHELXL-97 program.^{18b} Crystal parameters and information pertaining to data collection and refinement for all the structures are summarized in Table 1, whereas detailed descriptions are provided in the Supporting Information.

Results and Discussion

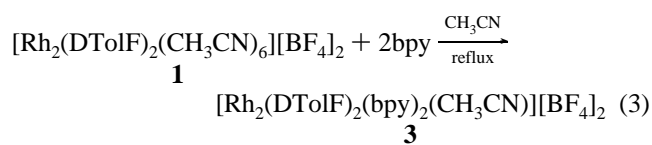
Syntheses. Compound **1** reacts with 1 equiv of bpy in CH_3CN at r.t. to afford a mixture of products (eq 1) as discerned by ^1H NMR spectroscopy (*vide infra*). The monosubstituted



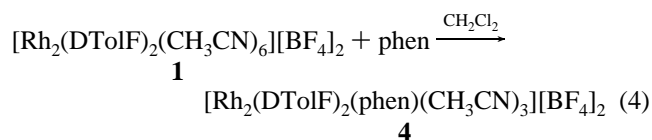
bpy product preferentially forms when acetone is used as the reaction solvent instead of CH_3CN (eq 2).



Compound **2** accounts for one set of bpy resonances observed in the ^1H NMR spectrum of the solid isolated from the reaction in CH_3CN at r.t. (*vide infra*). Under reflux conditions in CH_3CN , the binding of two bpy ligands to a single dirhodium core results in the formation of **3** (eq 3).



Equation 4 summarizes the addition of 1 equiv of phen in CH_2Cl_2 to produce **4**.



The addition of a second equiv of phen to the dirhodium

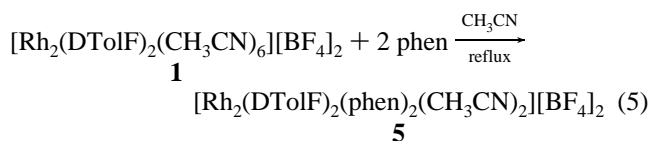
Table 2. Selected Bond Distances (Å) and Angles (deg) for $[\text{Rh}_2(\text{DTolF})_2(\text{bpy})(\text{CH}_3\text{CN})_3][\text{BF}_4]_2 \cdot (\text{CH}_3)_2\text{CO}$ (**2a**)

| bonds | | | |
|-------------------|-----------|-------------------|------------|
| Rh(1)–Rh(2) | 2.5783(3) | Rh(2)–N(2B) | 1.997(2) |
| Rh(1)–N(2) | 2.107(3) | Rh(1)–N(1') | 2.051(2) |
| Rh(1)–N(1A) | 2.057(3) | Rh(2)–N(3) | 2.028(3) |
| Rh(2)–N(2A) | 2.025(3) | Rh(1)–N(1) | 2.035(2) |
| Rh(1)–N(1B) | 2.068(2) | Rh(2)–N(4) | 2.025(2) |
| angles | | | |
| N(1)–Rh(1)–N(1') | 79.93(10) | N(2)–Rh(1)–Rh(2) | 177.95(7) |
| N(1)–Rh(1)–N(1A) | 95.27(10) | N(2B)–Rh(2)–N(4) | 174.36(10) |
| N(1')–Rh(1)–N(1A) | 174.10(9) | N(2A)–Rh(2)–N(4) | 91.64(10) |
| N(1')–Rh(1)–N(1B) | 97.61(10) | N(2B)–Rh(2)–N(3) | 88.18(10) |
| N(1A)–Rh(1)–N(1B) | 87.02(10) | N(2A)–Rh(2)–N(3) | 175.13(10) |
| N(1)–Rh(1)–N(2) | 87.99(9) | N(4)–Rh(2)–N(3) | 89.63(10) |
| N(1A)–Rh(1)–N(2) | 94.57(10) | N(4)–Rh(2)–Rh(1) | 101.73(7) |
| N(1)–Rh(1)–Rh(2) | 89.97(7) | N(3)–Rh(2)–Rh(1) | 99.45(7) |
| N(1A)–Rh(1)–Rh(2) | 85.61(7) | C(1B)–N(1B)–Rh(1) | 116.89(19) |
| N(1B)–C(1B)–N(2B) | 123.6(3) | N(1A)–C(1A)–N(2A) | 124.0(3) |

Table 3. Selected Bond Distances (Å) and Angles (deg) for $[\text{Rh}_2(\text{DTolF})_2(\text{bpy})(\text{CH}_3\text{CN})_4][\text{BF}_4]_2$ (**2b**)

| bonds | | | |
|-------------------|-----------|-------------------|-----------|
| Rh(1)–Rh(2) | 2.638(3) | Rh(1)–Rh(2) | 2.638(3) |
| Rh(1)–N(1A) | 2.023(5) | Rh(2)–N(2B) | 2.032(6) |
| Rh(1)–N(6) | 2.028(8) | Rh(2)–N(2A) | 2.039(6) |
| Rh(1)–N(1B) | 2.033(8) | Rh(2)–N(1) | 2.059(6) |
| Rh(1)–N(5) | 2.047(6) | Rh(2)–N(1') | 2.067(6) |
| Rh(1)–N(3) | 2.316(5) | Rh(2)–N(4) | 2.208(7) |
| angles | | | |
| N(1A)–Rh(1)–N(6) | 178.6(3) | N(2B)–Rh(2)–N(1) | 174.4(3) |
| N(1A)–Rh(1)–N(1B) | 88.4(3) | N(2A)–Rh(2)–N(1) | 96.3(2) |
| N(1A)–Rh(1)–N(5) | 91.9(2) | N(2A)–Rh(2)–N(1') | 174.7(3) |
| N(1B)–Rh(1)–N(5) | 177.6(3) | N(1)–Rh(2)–N(1') | 79.0(2) |
| N(1A)–Rh(1)–N(3) | 93.9(2) | N(2B)–Rh(2)–N(4) | 99.4(3) |
| N(6)–Rh(1)–N(3) | 85.6(3) | N(2A)–Rh(2)–N(4) | 96.0(3) |
| N(1A)–Rh(1)–Rh(2) | 84.04(17) | N(1)–Rh(2)–N(4) | 83.6(2) |
| N(6)–Rh(1)–Rh(2) | 96.5(2) | N(2B)–Rh(2)–Rh(1) | 85.18(16) |
| N(5)–Rh(1)–Rh(2) | 96.78(16) | N(1)–Rh(2)–Rh(1) | 91.6(2) |
| N(1A)–C(1A)–N(2A) | 124.3(6) | N(1B)–C(1B)–N(2B) | 125.1(10) |

core to yield $[\text{Rh}_2(\text{DTolF})_2(\text{phen})_2(\text{CH}_3\text{CN})_2][\text{BF}_4]_2$ (**5**) (eq 5) occurs only under refluxing conditions analogous to those required to prepare compound **3**.



Reaction of **2a** with 9-EtAH and 9-EtGH produced X-ray quality crystals of the previously reported compounds $[\text{Rh}_2(\text{DTolF})_2(9\text{-EtAH})_2(\text{CH}_3\text{CN})][\text{BF}_4]_2$ ¹¹ and $[\text{Rh}_2(\text{DTolF})_2(9\text{-EtGH})_2(\text{CH}_3\text{CN})_2][\text{BF}_4]_2$,^{11b} respectively.

Description of Structures. ORTEP representations of the cations in **2a**, **2b**, **3**, and **4** are depicted in Figures 1, 3, 4, and 5, respectively. Important bond distances and angles are listed in Tables 2–5.

$[\text{Rh}_2(\text{DTolF})_2(\text{bpy})(\text{CH}_3\text{CN})_3][\text{BF}_4]_2 \cdot (\text{CH}_3)_2\text{CO}$ (**2a**). Compound **2a** crystallizes in the monoclinic space group $P2_1/n$ with two $[\text{BF}_4]^-$ anions and one molecule of interstitial acetone. The most notable feature of **2a** is the presence of a single *ax* CH_3CN molecule {distance Rh(1)–N(2) = 2.107(3) Å; Figure 1}. The fact that the *ax* position of Rh(2) is unoccupied is a rather unusual finding, but it is not

(17) SAINT and SADABS programs in the SHELXTL software; Bruker AXS, Inc.: Madison, WI.

(18) (a) Sheldrick, G. M. *SHELXS-97*; University of Göttingen: Göttingen, Germany, 1990. (b) Sheldrick, G. M. *SHELXL-97, Program for refining crystal structures*; University of Göttingen: Göttingen, Germany, 1997.

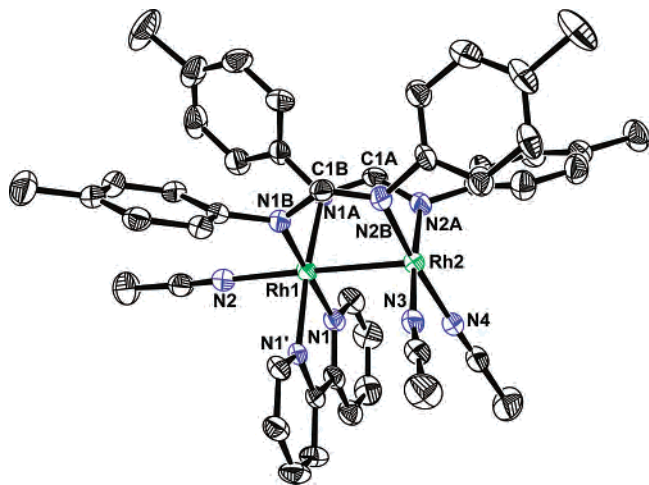
(19) *TEXSAN-TEXRAY Structure Analysis Package*; Molecular Structure Corporation: The Woodlands, TX, 1985. (b) Sheldrick, G. M. *SHELXS-86*; University of Göttingen: Göttingen, Germany, 1986.

Table 4. Selected Bond Distances (Å) and Angles (deg) for $[\text{Rh}_2(\text{DTolF})_2(\text{bpy})_2(\text{CH}_3\text{CN})][\text{BF}_4]_2$ (**3**)

| bonds | | | |
|--------------------|------------|--------------------|------------|
| Rh(1)–N(3B) | 2.024(3) | Rh(2)–N(1B) | 2.037(4) |
| Rh(1)–N(1A') | 2.032(3) | Rh(2)–N(1B') | 2.046(3) |
| Rh(1)–N(3A) | 2.031(3) | Rh(2)–N(4A) | 2.066(3) |
| Rh(1)–N(1A) | 2.041(3) | Rh(2)–N(4B) | 2.075(3) |
| Rh(1)–Rh(2) | 2.5821(5) | Rh(2)–N(1) | 2.116(4) |
| angles | | | |
| N(3B)–Rh(1)–N(1A') | 174.28(14) | N(1B')–Rh(2)–N(4A) | 99.07(14) |
| N(3B)–Rh(1)–N(3A) | 88.33(14) | N(4A)–Rh(2)–N(4B) | 87.21(14) |
| N(1A')–Rh(1)–N(3A) | 94.32(13) | N(1B)–Rh(2)–N(1) | 89.04(14) |
| N(3B)–Rh(1)–N(1A) | 96.55(14) | N(4A)–Rh(2)–N(1) | 90.21(14) |
| N(1A')–Rh(1)–N(1A) | 80.60(14) | N(1B)–Rh(2)–Rh(1) | 94.62(10) |
| N(3A)–Rh(1)–N(1A) | 174.55(14) | N(4A)–Rh(2)–Rh(1) | 86.10(10) |
| N(3B)–Rh(1)–Rh(2) | 85.06(10) | N(1A)–Rh(1)–Rh(2) | 98.60(10) |
| N(1)–Rh(2)–Rh(1) | 175.71(11) | N(1B)–Rh(2)–N(4A) | 178.70(15) |
| N(4A)–C(7A)–N(3A) | 123.5(4) | N(4B)–C(7B)–N(3B) | 123.8(4) |

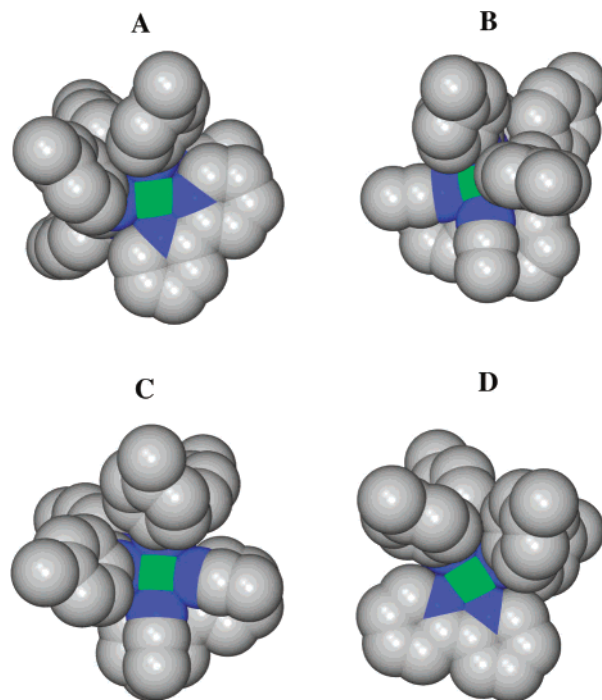
Table 5. Selected Bond Distances (Å) and Angles (deg) for $[\text{Rh}_2(\text{DTolF})_2(\text{phen})(\text{CH}_3\text{CN})_3][\text{BF}_4]_2 \cdot 2\text{C}_2\text{H}_5\text{OC}_2\text{H}_5$ (**4**)

| bonds | | | |
|-------------------|-----------|-------------------|-----------|
| Rh(1)–N(2) | 2.053(1) | Rh(1)–Rh(2) | 2.5808(2) |
| Rh(1)–N(1A) | 2.059(1) | Rh(2)–N(2B) | 2.009(2) |
| Rh(1)–N(1) | 2.060(2) | Rh(2)–N(2A) | 2.011(1) |
| Rh(1)–N(1B) | 2.069(2) | Rh(2)–N(5) | 2.028(2) |
| Rh(1)–N(3) | 2.128(2) | Rh(2)–N(4) | 2.036(1) |
| angles | | | |
| N(2)–Rh(1)–N(1A) | 177.40(8) | N(3)–Rh(1)–Rh(2) | 173.92(6) |
| N(2)–Rh(1)–N(1) | 80.83(8) | N(2B)–Rh(2)–N(5) | 175.72(8) |
| N(1A)–Rh(1)–N(1) | 98.11(8) | N(2A)–Rh(2)–N(5) | 89.51(8) |
| N(1A)–Rh(1)–N(1B) | 87.40(8) | N(2B)–Rh(2)–N(4) | 90.77(8) |
| N(1)–Rh(1)–N(1B) | 172.08(7) | N(5)–Rh(2)–N(4) | 88.61(8) |
| N(2)–Rh(1)–N(3) | 88.55(7) | N(2B)–Rh(2)–Rh(1) | 84.61(6) |
| N(1A)–Rh(1)–N(3) | 93.72(7) | N(5)–Rh(2)–Rh(1) | 99.67(5) |
| N(1)–Rh(1)–N(3) | 84.53(8) | N(2)–Rh(1)–Rh(2) | 91.03(5) |
| N(1)–Rh(1)–Rh(2) | 89.41(5) | N(1A)–Rh(1)–Rh(2) | 86.58(6) |
| N(1A)–C(1A)–N(2A) | 123.3(2) | N(1B)–C(2A)–N(2B) | 123.4(2) |

**Figure 1.** ORTEP representation of compound **2a** drawn at the 50% probability level. Hydrogen atoms are omitted for clarity.

unprecedented for dirhodium compounds; it has been observed for $[\text{Rh}_2(\text{DTolF})_2(9\text{-EtAH})_2(\text{CH}_3\text{CN})][\text{BF}_4]_2$,^{11b} $\text{Rh}_2(\text{DPhF})_4(\text{CH}_3\text{CN})$ (DPhF = *N,N'*-diphenylformamidinate),²⁰ $[\text{Rh}_2(\text{DTolF})_4(\text{H}_2\text{O})]^{+2}$,²¹ $[\text{Rh}_2(\text{DTolTA})_2(\text{bpy})(\text{CH}_3\text{CN})_3](\text{PF}_6)_2$ (DTolTA = di-*p*-tolyltriazine),²² and $\text{Rh}_2(\text{TiPB})_4(\text{CH}_3\text{CN})$

(20) (a) Bear, J. L.; Yao, C.-L.; Lifsey, R. S.; Korp, J. D.; Kadish, K. M. *Inorg. Chem.* **1991**, *30*, 336. (b) Piraino, P.; Bruno, G.; Schiavo, S. L.; Laschi, F.; Zanello, P. *Inorg. Chem.* **1987**, *26*, 2205.

**Figure 2.** Space-filling models for the cation of **2a** after removal of the axial solvent molecules viewed from the *ax* site with (A) *ax* solvent, (B) no solvent molecule, and (C and D) space-filling models for the cation of **2b** viewed from the *ax* sites after removal of *ax* solvent molecules.

(TiPB = triisopropylbenzoate)²³ and has been attributed to steric and electronic factors.^{20,22} The space-filling models for the cation of **2a** viewed from each *ax* site (Figure 2, A and B) indicate that subtle differences in the conformations of the $[\text{DTolF}]^-$ bridging groups cause the unoccupied *ax* site to be less accessible to solvent molecules. In contrast, the space-filling models for the cation of **2b**, which has two *ax* ligands, indicate that both *ax* sites are equally accessible (Figure 2, C and D).

In **2a**, the Rh–Rh bond distance is 2.5783(3) Å, which is slightly longer than the corresponding bond distance of the related compound $[\text{Rh}_2(\text{O}_2\text{CCH}_3)_2(\text{bpy})(\text{CH}_3\text{CN})_4]^{2+}$ {2.5395(8) Å}.^{15b} Compound **2a** possesses an *eq–eq* bpy molecule with Rh–N bond distances of 2.035(2) Å and 2.051(2) Å, which are ~0.04 Å longer than that reported for $[\text{Rh}_2(\text{O}_2\text{CCH}_3)_2(\text{bpy})(\text{CH}_3\text{CN})_4]^{2+}$ {2.001(6) Å}; this lengthening is attributed to the stronger *trans* influence of the formamidinate as compared to the acetate ligands.^{15b} The pyridyl rings are slightly twisted by 2.8° and the two $[\text{DTolF}]^-$ ligands are twisted by 14.8° and 16.8° from the eclipsed orientation as compared to 19° for $[\text{Rh}_2(\text{DTolF})_2(\text{CH}_3\text{CN})_6](\text{BF}_4)_2$ (**1**).¹¹ The Rh–N distances of 2.057(3) Å and 2.068(2) Å for the $[\text{DTolF}]^-$ anions coordinated to Rh(1) are longer than the Rh–N distances for Rh(2) {1.997(2) Å and 2.025(3) Å}. The differences in the Rh–N $[\text{DTolF}]^-$ bond

(21) Bruno, G.; Schiavo, S. L.; Tresoldi, G.; Piraino, P. *Inorg. Chim. Acta* **1992**, *196*, 131.

(22) Connelly, N. G.; Einig, T.; Herbosa, G. G.; Hopkins, P. M.; Mealli, C.; Orpen, A. G.; Rosair, G. M.; Viguri, F. *J. Chem. Soc., Dalton Trans.* **1994**, 2025.

(23) Cotton, F. A.; Hillard, E. A.; Liu, C. Y.; Murillo, C. A.; Wang, W.; Wang, X. *Inorg. Chim. Acta* **2002**, *337*, 233.

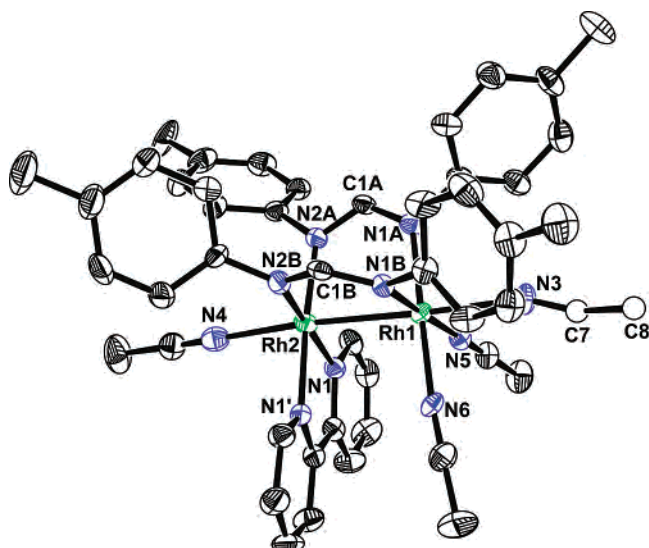


Figure 3. ORTEP representation of compound **2b** drawn at the 50% probability level. Hydrogen atoms are omitted for clarity. Atoms C7 and C8 are drawn as spheres of arbitrary size due to their large thermal parameters.

distances are attributed to the presence of the *trans* bpy ligand and the *ax* acetonitrile coordinated to Rh(1).

[Rh₂(DTolF)₂(bpy)(CH₃CN)₄][BF₄]₂ (2b**).** Compound **2b** crystallizes in the monoclinic space group *P*2₁/*n* with the asymmetric unit consisting of the entire cation and two [BF₄][−] anions. The close packing arrangement of the [BF₄][−] ions to an *ax* CH₃CN causes the latter ligand of Rh(1) to be at an 151(4)° angle (Figure 3). The unusual binding of the *ax* CH₃CN molecule is also reflected by the long Rh(1)–N(3) bond distance of 2.316(5) Å as compared to the *ax* CH₃CN solvent molecule of Rh(2) {Rh–N bond distance 2.208(7) Å}. The *ax* Rh–N distances in **2b** are significantly longer than those in **2a** {2.107(3) Å}.

In the cation of **2b**, the chelating *eq*–*eq* bpy ligand has the pyridyl rings twisted by 2.2°. The Rh–N bond distances of the bpy ligand are 2.059(6) Å and 2.067(6) Å, which are comparable to those in **2a**. As expected, the *ax* Rh–N bond distances {2.208(7) Å and 2.316(5) Å} are longer than the *eq* Rh–N bond distances {2.028(8) Å and 2.047(6) Å}. The Rh–Rh bond distance is 2.638(3) Å, which is significantly longer than that in **2a** {2.5783(3) Å} and related compounds.^{15b,c} The lengthening of the Rh–Rh bond may be attributed to the presence of the *ax* CH₃CN molecule bound to Rh(2), a site that is unoccupied in **2a**. The [DTolF][−] groups are twisted from the eclipsed conformation by 7.9° and 8.4°, in contrast to those in **2a** which exhibit significantly larger twist angles {14.8° and 16.8°}.

[Rh₂(DTolF)₂(bpy)₂(CH₃CN)][BF₄]₂ (3**).** Compound **3** crystallizes in the monoclinic space group *P*2₁/*a*. As in the case of **2a**, the dirhodium cation in **3** possesses only one *ax* CH₃CN molecule with a Rh(2)–N(1) bond distance of 2.116(4) Å (Figure 4). The Rh–Rh bond distance is 2.5821(5) Å, which is longer than the metal–metal bond distances in [Rh₂(O₂CCH₃)₂(bpy)₂(CH₃CN)₂][PF₆]₂ {2.548(1) Å} and Rh₂(O₂CCF₃)₄(bpy)₂ {2.570(6) Å}.^{15c} The cation consists of two chelating *eq*–*eq* groups attached to two Rh atoms in a *syn* disposition. The average Rh–N distance for the *eq*–*eq*

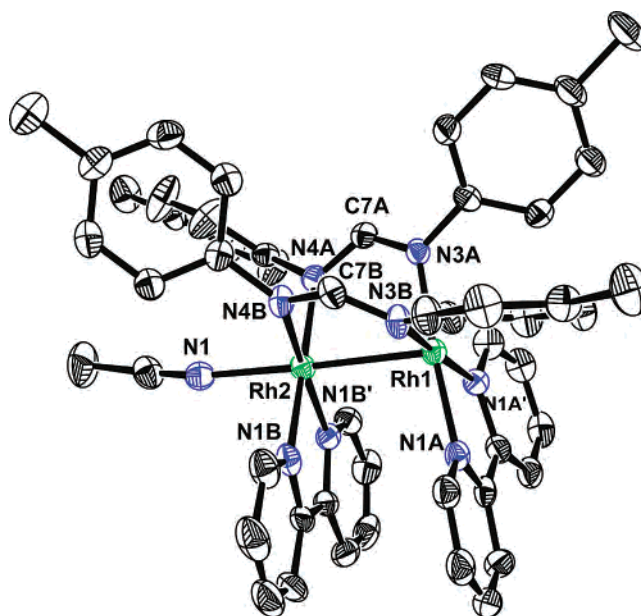


Figure 4. ORTEP representation of compound **3** drawn at the 50% probability level. Hydrogen atoms are omitted for clarity.

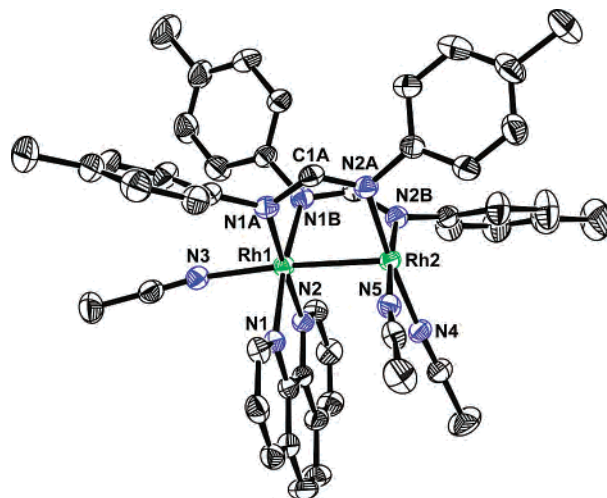


Figure 5. ORTEP representation of compound **4** drawn at the 50% probability level. Hydrogen atoms are omitted for clarity.

bound bpy groups {2.0341(4) Å} is comparable to the corresponding distances in **2a** and **2b**.^{15c} The unfavorably short bpy···bpy contacts in **3** are alleviated by a splaying of the bpy groups away from the center of the molecule, resulting in a dihedral angle of 14.8° between the N(1B), N(1B'), N(4B), N(4A) and N(1A), N(1A'), N(3B), N(3A) least-squares planes; this angle is comparable to those reported for [Rh₂(O₂CCH₃)₂(bpy)₂(CH₃CN)₂]²⁺ (15.8°) and Rh₂(O₂CCF₃)₄(bpy)₂ (11.7°).^{15c}

[Rh₂(DTolF)₂(phen)(CH₃CN)₃][BF₄]₂·2C₂H₅OC₂H₅ (4**).** Compound **4** crystallizes in the triclinic space group *P*1̄ with two molecules of diethyl ether. As in the case of **2a**, the *ax* site of Rh(2) is not occupied (Figure 5). The *eq*–*eq* phen ligand is bound to Rh(1) with Rh–N distances of 2.053(1) Å and 2.060(2) Å. The pyridyl rings of the phen ligands are twisted out of the plane by 1.5°. The Rh–Rh bond distance of 2.5808(2) Å is comparable to the analogous distance in **2a**. As in the case of **2a**, the Rh–N bond distances of the

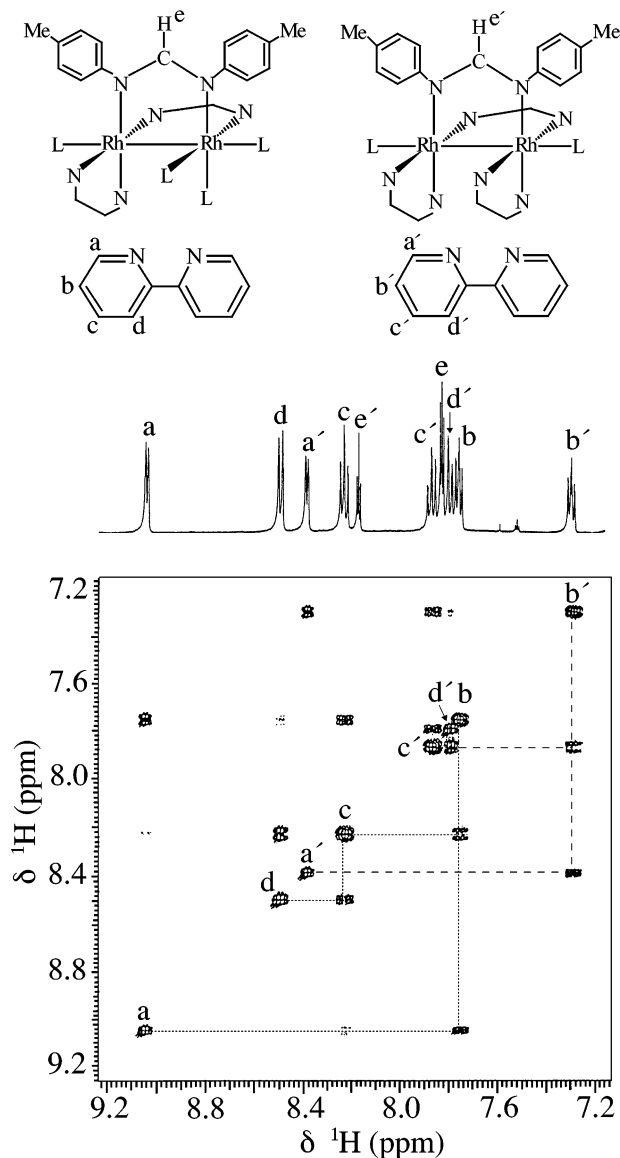


Figure 6. 2D COSY [^1H - ^1H] NMR spectrum in $\text{CD}_3\text{CN}-d_3$ depicting the aromatic region of the mixture of compounds **2** and **3** produced during the reaction of **1** with bpy in CH_3CN at r.t. (eq 1). The protons that belong to the mono- and bis-bpy dirhodium adducts are labeled a, b, c, d, e and a', b', c', d', e', respectively.

$[\text{DTolF}]^-$ ligands *trans* to the N–N chelate are lengthened with respect to those *trans* to the CH_3CN ligands.

^1H NMR Spectroscopy. The reaction of **1** with bpy at r.t. in CH_3CN yields a mixture of **2** and **3**. The ^1H NMR spectrum of the reaction mixture initially prompted us to postulate that two different mono-bpy isomers were present, namely the dirhodium formamidinate adducts with *eq*–*eq* or *ax*–*eq* binding modes for bpy, but the 1D ^1H NMR spectra of pure crystals of **2** and **3** allowed for the definitive assignment of the 2D NMR spectrum. The 2D ^1H NMR spectrum of the mixture in $\text{CD}_3\text{CN}-d_3$ depicts two independent sets of four coupled protons (a, b, c, d and a', b', c', d') that can be attributed to the bpy protons of two different adducts, namely **2** and **3** (Figure 6). The majority of the

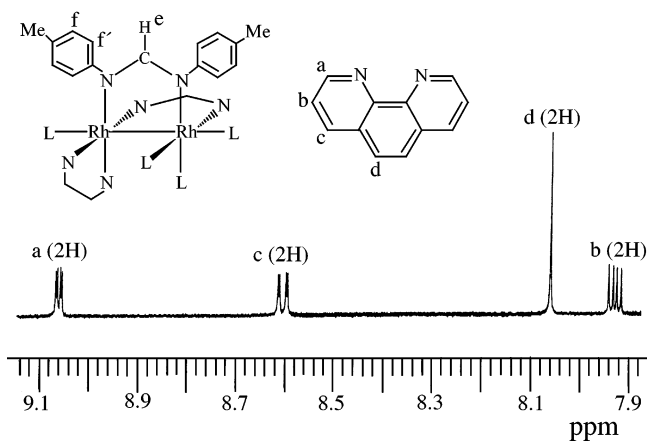


Figure 7. ^1H NMR spectrum of $[\text{Rh}_2(\text{DTolF})_2(\text{phen})(\text{CH}_3\text{CN})_3][\text{BF}_4]_2$ (**4**) in $\text{CD}_3\text{CN}-d_3$.

resonances are split into multiplets due to three-bond coupling to neighboring protons of the same ring. Each of these sets is shifted from the corresponding resonances of the unbound ligand, indicating binding of the latter to the dirhodium unit.

The set of bpy resonances a, b, c, and d at 9.06, 7.77, 8.24, and 8.50 ppm, respectively, with the expected integral ratio, is attributed to the bpy protons of $[\text{Rh}_2(\text{DTolF})_2(\text{bpy})(\text{CH}_3\text{CN})_4][\text{BF}_4]_2$ (**2**) (Figure 6A). Even though the four bpy resonances suggest that the two pyridyl rings are equivalent, a careful inspection of the cross-peaks in the 2D NMR spectrum reveals the presence of overlapping multiplets due to the nonequivalent bpy rings (consistent with C_s symmetry). The ^1H NMR spectrum for **2** resembles that of $[\text{Rh}_2(\text{O}_2\text{CCH}_3)_2(\text{bpy})(\text{CH}_3\text{CN})_4]^{2+}$ ^{15b} in the number and splitting pattern of the resonances, an expected finding since both the compounds possess *eq*–*eq* chelating bpy rings and differ only in the bridging groups. The triplet labeled e at 7.83 ppm is assigned to the bridge NCHN protons of the $[\text{DTolF}]^-$ groups (splitting is due to ^{103}Rh coupling) and is in a 1:1 ratio with each of the bpy resonances. The methyl protons of the $[\text{DTolF}]^-$ groups resonate at 2.22 ppm, whereas the *eq* coordinated CH_3CN groups give rise to a resonance at 2.25 ppm. The ^1H NMR spectrum of $[\text{Rh}_2(\text{DTolF})_2(\text{bpy})(\text{CH}_3\text{CN})_4]^{2+}$ has been previously reported in the literature.¹⁶

The ^1H NMR spectrum of $[\text{Rh}_2(\text{DTolF})_2(\text{bpy})_2(\text{CH}_3\text{CN})][\text{BF}_4]_2$ (**3**) (Figure 6B) (with effective C_{2v} symmetry) accounts for the remaining set of four bpy resonances a', b', c', and d' at 8.38, 7.29, 7.86, and 7.79 ppm, respectively, in the expected integral ratio. The triplet at 8.17 ppm (labeled e') is assigned to the bridge NCHN protons of the $[\text{DTolF}]^-$ groups (splitting is due to ^{103}Rh coupling) and is in a 1:2 ratio with the bpy resonances, thus confirming that two bpy ligands are bound to the dirhodium core. The $[\text{DTolF}]^-$ methyl protons give rise to a singlet at 2.23 ppm. The *ax* CH_3CN ligands for both **2** and **3** are in rapid exchange with the bulk solvent on the NMR time-scale and are observed at 1.95 ppm. The ^1H NMR spectrum for $[\text{Rh}_2(\text{DTolF})_2(\text{bpy})_2(\text{CH}_3\text{CN})_2]^{2+}$ has been previously reported in the literature.¹⁶

The ^1H NMR spectrum of $[\text{Rh}_2(\text{DTolF})_2(\text{phen})(\text{CH}_3\text{CN})_3][\text{BF}_4]_2$ (**4**) is in accord with the solid-state structure (Figure 7). The axially coordinated CH_3CN ligands resonate at 1.95

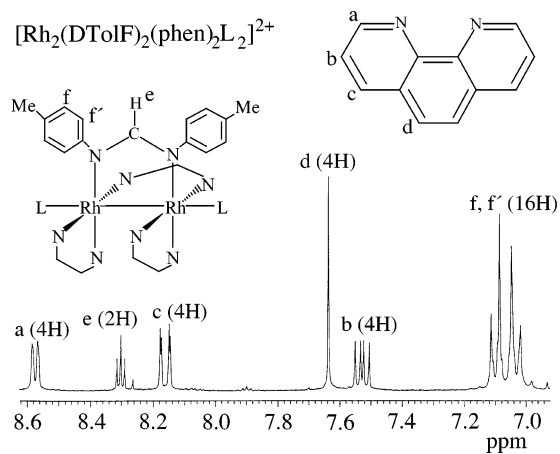


Figure 8. ^1H NMR spectrum of $[\text{Rh}_2(\text{DTolF})_2(\text{phen})_2(\text{CH}_3\text{CN})_2][\text{BF}_4]_2$ (**5**) in $\text{CD}_3\text{CN}-d_3$.

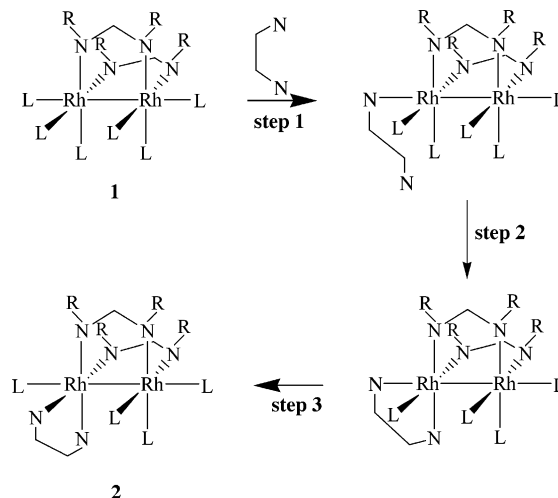
ppm (chemical shift for free $\text{CD}_3\text{CN}-d_3$) due to rapid exchange with the bulk solvent on the NMR time scale. Unlike the mono-bpy analogue **2**, for which the *eq* CH_3CN protons are observed at 2.25 ppm, the corresponding protons in **4** resonate further downfield at 2.51 ppm. The $[\text{DTolF}]^-$ methyl and aromatic protons give rise to resonances at 2.25 and 6.99 ppm, respectively. The phen protons are observed at 7.92 (b), 8.06 (d), 8.60 (c), and 9.05 (a) ppm.

Although it was not possible to resolve the X-ray crystal structure of $[\text{Rh}_2(\text{DTolF})_2(\text{phen})_2(\text{CH}_3\text{CN})_2][\text{BF}_4]_2$ (**5**), ^1H NMR spectroscopy proved useful in discerning the molecular structure. The ^1H NMR spectrum of **5** (Figure 8) indicates that it resembles **3**. Four resonances at 7.53 (b), 7.63 (d), 8.15 (c), and 8.57 (a) ppm are attributed to the phen ligand, whereas a triplet at 8.30 (e) ppm which is assigned to the bridge NCHN protons of $[\text{DTolF}]^-$, is in a 1:2 ratio with each set of the four phen resonances. The *ax* CH_3CN is observed at 1.95 ppm, but no downfield resonances attributable to *eq* CH_3CN are observed. The $[\text{DTolF}]^-$ methyl protons resonate at 2.24 ppm. The previous data are in accord with a dirhodium adduct that has two phen ligands coordinated in an *eq-eq* fashion.

The single-crystal X-ray structural characterizations of **2** and **4** revealed the presence of N–N ligands bound only in an *eq-eq* fashion to the dirhodium formamidinate core, unlike the dirhodium carboxylate derivatives for which *ax-eq* as well as *eq-eq* binding modes of the N–N ligands have been observed.^{15b} The fact that no *ax-eq* dirhodium formamidinate adducts are observed may be attributed to the strong *trans* influence of the formamidinate groups which renders the CH_3CN groups more labile, opening thus the *eq* positions to the incoming N–N ligands. It is logical to postulate for the dirhodium formamidinate compounds a mechanism similar to that of the carboxylates,^{15b} but it is expected that the *ax-eq* intermediate formed during step 2 swiftly proceeds to step 3 to produce the final product **2** (Chart 2).

Electrochemistry of 2, 3, 4, and 5. A summary of the half-wave potentials for the bis-formamidinate dirhodium compounds is provided in Table 6. The cyclic voltammogram for $[\text{Rh}_2(\text{DTolF})_2(\text{bpy})(\text{CH}_3\text{CN})_4]^{2+}$ in CH_3CN consists of a

Chart 2. Proposed Sequence of Events Involved in the Reactions of Dirhodium Bis-formamidinate Compounds with N–N Chelating Ligands^a



^a Final adduct **2** has the N–N chelate attached to the dirhodium core in an *eq-eq* binding mode.

Table 6. Cyclic Voltammetric Data for Bis-acetate and Bis-formamidinate Dirhodium Compounds in CH_3CN ^a

| compound | $E_{1/2}$ (ox) ₁ | $E_{1/2}$ (ox) ₂ | $E_{1/2}$ (red) ₁ | $E_{1/2}$ (red) ₂ |
|---|--------------------------------|--------------------------------|---------------------------------|---------------------------------|
| $[\text{Rh}_2(\text{OAc})_2(\text{bpy})_2(\text{CH}_3\text{CN})]^{2+ b}$ | | | −0.89 | |
| $[\text{Rh}_2(\text{OAc})_2(\text{phen})_2(\text{CH}_3\text{CN})_2]^{2+ b}$ | | | −0.83 | |
| $[\text{Rh}_2(\text{DTolF})_2(\text{CH}_3\text{CN})_6]^{2+}$ | +1.00 ^c | | −0.47 ^d | −1.30 |
| $[\text{Rh}_2(\text{DTolF})_2(\text{bpy})(\text{CH}_3\text{CN})_3]^{2+}$ | +1.00 | | −0.44 | −1.17 |
| $[\text{Rh}_2(\text{DTolF})_2(\text{bpy})_2(\text{CH}_3\text{CN})]^{2+}$ | +1.02 | | −0.50 ^d | −1.30 ^d |
| $[\text{Rh}_2(\text{DTolF})_2(\text{phen})(\text{CH}_3\text{CN})_4]^{2+}$ | +1.07 ^c | +1.50 ^c | −0.53 ^d | −1.42 ^d |
| $[\text{Rh}_2(\text{DTolF})_2(\text{phen})_2(\text{CH}_3\text{CN})_2]^{2+}$ | +1.05 ^c | +1.57 ^c | −0.91 | −1.47 ^d |

^a $E_{1/2}$ values in volts vs Ag/AgCl in CH_3CN with 0.1 M tetra-*n*-butylammonium tetrafluoroborate as supporting electrolyte. ^b Values reported in ref 15c. ^c $E_{p,a}$ value; $i_{p,c}/i_{p,a} \neq 1$. ^d $E_{p,c}$ value; $i_{p,c}/i_{p,a} \neq 1$.

reversible oxidation at $E_{1/2} = +1.0$ V and a reversible reduction at $E_{1/2} = -0.44$ V. A quasi-reversible reduction process occurs at $E_{p,c} = -1.19$ V with an associated return wave of $E_{p,a} = -1.15$ V ($i_{p,c}/i_{p,a} = 1.3$). The electrochemical behavior of $[\text{Rh}_2(\text{DTolF})_2(\text{bpy})_2(\text{CH}_3\text{CN})]^{2+}$ (cation of **3**) is similar to that of $[\text{Rh}_2(\text{DTolF})_2(\text{bpy})(\text{CH}_3\text{CN})_4]^{2+}$ in CH_3CN . Compound **3** exhibits two quasi-reversible reductions at $E_{p,c} = -0.50$ and -1.30 V with associated return waves at $E_{p,a} = -0.37$ V ($i_{p,c}/i_{p,a} = 2$) and -1.2 V ($i_{p,c}/i_{p,a} = 2.5$), respectively.

For the cation $[\text{Rh}_2(\text{DTolF})_2(\text{phen})(\text{CH}_3\text{CN})_3]^{2+}$ of **4**, two quasi-reversible anodic processes are observed at +1.07 and +1.50 V. In addition to the two oxidation processes, the compound gives rise to two quasi-reversible reductions at $E_{p,c} = -0.53$ and -1.42 V. The return waves associated with these processes occur at $E_{p,a} = -0.43$ and -1.36 V with $i_{p,c}/i_{p,a}$ ratios of 1.7 and 1.9, respectively. The bis-phenanthroline cation $[\text{Rh}_2(\text{DTolF})_2(\text{phen})_2(\text{CH}_3\text{CN})_2]^{2+}$ in **5** exhibits oxidation processes that are similar to **4** in CH_3CN . Two quasi-reversible oxidations occur at $E_{p,a} = +1.05$ and +1.57 V, respectively, with the associated return waves at $E_{p,c} = +0.99$ and +1.43 V and $i_{p,a}/i_{p,c}$ ratios of 1.5 and 1.8, respectively. A reversible cathodic process for the cation of **5** occurs at $E_{1/2} = -0.91$ V, and two quasi-reversible processes occur at $E_{p,c} = -1.47$ V and $E_{p,c} = -1.89$ V,

respectively. The corresponding return wave for the first reduction process is at $E_{p,a} = -1.43$ V with an $i_{p,c}/i_{p,a}$ ratio of 2.0.

A comparison of the electrochemical data of the dirhodium formamidinate with the corresponding acetate compounds (Table 6) reveals that the presence of the formamidinate groups renders these compounds more easily oxidized since the $[\text{Rh}_2(\text{O}_2\text{CR})_2(\text{bpy})_2\text{CH}_3\text{CN})_2]^{2+}$ (R = Me, Et, Ph) adducts do not undergo oxidation processes, but exhibit only a single-electron reduction process occurring at ~ -0.90 V. Similarly, the redox properties of the cation in **5** are different from those of the analogous acetate compound $[\text{Rh}_2(\text{O}_2\text{CCH}_3)_2(\text{phen})_2(\text{CH}_3\text{CN})_2]^{2+}$, which is reported to undergo a reversible reduction at $E_{1/2} = -0.83$ V, but no oxidation processes.^{15c} Although the formamidinate bridging groups make the compounds more accessible to oxidation and reduction processes, the cyclic voltammetry measurements confirm persistence of the dirhodium core in solution. Preliminary results indicate that these compounds bind covalently to their biological targets (DNA or enzymes) and thus are unlikely to exhibit carcinostatic activity through a redox mechanism.

Conclusion

The reactions of the dirhodium bis-formamidinate compounds with N–N ligands (bpy or phen) lead to adducts with the *eq–eq* sites occupied by the chelating ligands, in contrast to the corresponding carboxylate derivatives which form *ax–eq* as well as *eq–eq* adducts. The different behavior of

the two classes of dirhodium compounds may be attributed to the strong *trans* influence of the bridging formamidinate ligands which labilize the *eq* groups across from them. A notable feature of the majority of the adducts reported herein is the presence of one *ax* ligand only, a finding that may be attributed to steric and electronic factors. The binding of N–N chelates to the formamidinate cation $[\text{Rh}_2(\text{DTolF})_2(\text{CH}_3\text{CN})_6]^{2+}$ takes place in a manner that is very similar to that of the dirhodium tetracarboxylate compounds and provides a useful model for the binding of adjacent DNA bases to the dirhodium core.^{11,12,15} The robust nature of the formamidinate compounds and their promising biological activity render them excellent candidates for further binding studies with DNA oligonucleotides. Such studies are underway and will be reported in due course.

Acknowledgment. Dr. John Bacsa is gratefully acknowledged for the final stages of the refinement for the crystal structures of **2a** and **4**. K.R.D. thanks the Welch Foundation (A1449) for financial support and Johnson-Matthey for a generous loan of rhodium.

Supporting Information Available: Description of X-ray crystallography and structure solutions for **2a**, **2b**, **3**, and **4**; crystallographic data in CIF format for compounds **2a**, **2b**, **3**, and **4**. This material is available free of charge via the Internet at <http://pubs.acs.org>.

IC034737B